

Exploration of Genetic Overlap of Brain Phenotypes With Schizophrenia: Different Methods Provide Complementary Insights

Xiao Wu^{1,*}, Pravesh Parekh^{2,⊕}, Bochao Danae Lin¹, Lotta-Katrin Pries¹, Sinan Guloksuz^{1,3}, Bart P. F. Rutten¹, Ole A. Andreassen², David E. J. Linden^{1,4}, and Dennis van der Meer^{1,2,⊕}

¹Department of Psychiatry and Neuropsychology, Mental Health and Neuroscience Research Institute, Faculty of Health, Medicine and Life Sciences, Maastricht University, Maastricht, 6200 MD, The Netherlands; ²Centre for Precision Psychiatry, Division of Mental Health and Addiction, Oslo University Hospital and Institute of Clinical Medicine, University of Oslo, Oslo, 0316, Norway; ³Department of Psychiatry, Yale University School of Medicine, New Haven, CT 06511, United States; ⁴Division of Psychological Medicine and Clinical Neurosciences, School of Medicine, Cardiff University, Cardiff, CF24 4HQ, United Kingdom.

*To whom correspondence should be addressed: Xiao Wu, Department of Psychiatry and Neuropsychology, Mental Health and Neuroscience Research Institute, Faculty of Health, Medicine and Life Sciences, Maastricht University, Maastricht, Vijverdalseweg 1, 6224 GV, Maastricht, The Netherlands (xiao.wu@maastrichtuniversity.nl).

Background: Genetic studies have shown associations between genetic risk for schizophrenia and brain imaging phenotypes. However, prior studies focused on a single neuroimaging modality and/or employed methods that do not fully elucidate the shared genetic architecture between them, limiting our understanding of their complex genetic relationship.

Study Design: We used genome-wide association study summary statistics for schizophrenia alongside 37 brain measurements, selected based on adequate SNP-based heritability and representing structural, microstructural, and functional brain features derived from T1, diffusion tensor imaging (DTI), and resting-state functional magnetic resonance imaging (rs-fMRI). These were integrated with a clinical cohort (1065 cases, 1037 controls) to examine the polygenic overlap between schizophrenia and brain measurements. Polygenic overlap was assessed at genome-wide and individual locus levels through linkage disequilibrium score regression, polygenic scoring (PGS), bivariate MiXeR, and conjunctive false discovery rate.

Study Results: Schizophrenia showed weak genetic correlations with all brain measures ($r_g = -0.131$ to 0.146 ; $P_{FDR} = .069$ to $.019$), and no significant correlation with brain PGS. Nonetheless, a substantial proportion of causal variants with mixed effect direction were shared between schizophrenia and brain traits. Genetic correlations and polygenic scores showed significant positive associations with the proportion of shared variants with concordant effect direction. Additionally, we identified 218 loci shared with schizophrenia in T1, 138 in DTI, and 24 in rs-fMRI measures.

Conclusions: Our findings indicate shared genetic underpinnings between schizophrenia and brain structure and functional connectivity, emphasizing the necessity for complementary methodologies to investigate the genetic overlap between complex polygenic traits.

Key words: schizophrenia; genetics; brain MRI; genome-wide association study; pleiotropy; genetic overlap.

Introduction

Schizophrenia is a highly heritable brain disorder (60%–80% in twin studies) with a complex genetic architecture,¹ impacting about 24 million people worldwide.^{2,3} The prevailing “neurodevelopmental” model of schizophrenia posits that disrupted brain development in early life, influenced by genetic and environmental risk factors, is an important vulnerability factor for developing schizophrenia.⁴

Neuroimaging research consistently reports structural brain differences in individuals with schizophrenia, including widespread thinner cortex, reduced intracranial volume (ICV), smaller total surface area, and decreased volume of certain subcortical structures, such as the hippocampus and thalamus.^{5–8} Diffusion tensor imaging (DTI) studies highlight pronounced white matter microstructure abnormalities across various brain regions, especially reduced fractional anisotropy (FA).^{9–11} Additionally, large-scale functional network dysfunction correlates with clinical features of schizophrenia.^{12,13} Most of these brain phenotypes are not only heritable and polygenic^{14–18}

but are also observed in high-risk individuals and unaffected relatives of those with schizophrenia,¹⁹ suggesting that genetic risk factors for schizophrenia may be associated with brain structure and function.

Exploring the shared genetic architecture of schizophrenia and brain phenotypes could shed light on the underlying pathological mechanisms of schizophrenia, yet previous studies have shown inconsistent findings. For instance, Franke et al. reported no significant genetic correlations between schizophrenia and subcortical volume,²⁰ while others observed genetic overlap.^{21–23} These inconsistencies may be partly due to the fact that there are multiple methods to estimate genetic overlap between 2 traits, which differ in the way this overlap is quantified. Linkage disequilibrium score regression (LDSC) quantifies genome-wide genetic correlation,^{24–26} depending on consistent effect directions of shared genetic variants. However, schizophrenia and brain phenotypes have complex polygenic architectures, where some shared variants have a concordant effect direction (ie, increasing or decreasing schizophrenia risk and brain measures in both), while others have discordant effect direction (ie, increasing schizophrenia risk while decreasing brain measures, or in the opposite direction). Shared variants with mixed effect directions generate opposing genetic correlations, which may cancel out genome-wide, potentially leading to an underestimation of genetic correlation estimates.^{27,28} Polygenic score (PGS) assesses individual genetic predisposition by aggregating effects of genetic variants across the genome, reflecting the polygenic basis of traits like schizophrenia. Higher schizophrenia PGS has been correlated with lower global cortex thickness,^{29,30} difference in regional brain volumes,^{31,32} and difference in functional connectivity.^{33,34} Brain imaging-derived PGS could identify individuals at high risk for schizophrenia.³⁵ Furthermore, Mendelian randomization analyses suggest that structural brain measures causally influence schizophrenia risk.^{36,37} Yet, similar to LDSC, PGS is limited by the fact that the impact of shared variants with mixed effect directions gets lost when summed together.

Another approach, bivariate Gaussian mixture modeling, implemented by the MiXeR tool, addresses these limitations by estimating the overall amount of shared causal variants, regardless of the effect directions.^{38,39} This approach estimates the amount of shared and trait-specific causal variants and the proportion of shared variants with concordant effect direction. The application of MiXeR has found subcortical brain volumes and average brain FA share causal variants with schizophrenia.²⁶ However, above methods do not pinpoint the location of shared variants. The conjunctive false discovery rate (conjFDR) approach leverages pleiotropy,^{40,41} where a single variant is associated with multiple distinct phenotypes, to enhance the power of genome-wide association study (GWAS) summary statistics and facilitate the identification of shared genetic loci. Applying conjFDR to schizophrenia has identified overlapping variants with

brain phenotypes, including subcortical volume, ICV, and functional connectivity.⁴²

These approaches offer complementary insights into the shared genetic architecture of complex traits, yet most studies have used a limited range of methods and focused on a single imaging modality. Combining multiple modalities, such as T1, DTI, and resting-state functional magnetic resonance imaging (rs-fMRI), can provide modality-specific genetic signals⁴³ and deepen our understanding of the shared genetic architecture between schizophrenia and brain phenotypes. Our study combines these methodologies to explore the genetic overlap between schizophrenia and brain imaging phenotypes from T1, DTI, and rs-fMRI, using LDSC, PGS, and MiXeR to assess genome-wide genetic overlap and conjFDR to identify local genetic loci.

Methods

GWAS Datasets

We utilized GWAS summary statistics for schizophrenia from the Psychiatric Genomic Consortium wave 3.¹ Specifically, we used data from a meta-analysis of 53 386 individuals with schizophrenia and 77 258 healthy controls of European ancestry. GWAS data for multimodal brain imaging phenotypes were acquired from the UK Biobank via the Oxford Brain Imaging Genetics Server (BIG40, <https://open.win.ox.ac.uk/ukbiobank/big40/>).⁴⁴ This dataset included 33 224 healthy individuals with White European ancestry, with slight variations across different phenotypes. For T1 brain phenotypes, we selected global brain phenotypes and subcortical volumetric phenotypes generated using FreeSurfer software⁴⁴ to compare our results with previous research. We also included the weighted-mean FA of white matter tracts from probabilistic tractography for DTI phenotypes. Last, we incorporated brain rs-fMRI measures derived from independent component analysis of brain functional network nodes at a dimensionality of 25. As our focus was on comparing statistical methods for estimating genetic overlap, and bilateral brain phenotypes are typically highly correlated both phenotypically and genetically in healthy individuals,^{14,45} we restricted analyses to the left hemisphere phenotypes to reduce the burden of multiple testing. We screened the above brain measures with an additive genetic heritability (h^2) greater than 0.1 and a significance threshold below 0.05,^{46,47} resulting in the inclusion of 11 T1, 15 DTI, and 11 rs-fMRI phenotypes (Table 1 and Figure S1). All the GWAS utilized in this study were approved by relevant ethics committees, with detailed genotyping and phenotype data processing details documented in the respective publications.^{44,48}

Individual-Level Datasets for PGS Calculation

For the PGS analysis, we employed genotype and phenotype data from a clinical cohort within Work-package

Table 1. Brain Phenotypes Included in the Study.

Modality	Brain phenotypes	h^2 (mean)	h^2 (SE)
T1	Volume of Thalamus-Proper (L)	0.278	0.024
T1	Volume of caudate (L)	0.349	0.027
T1	Volume of putamen (L)	0.321	0.027
T1	Volume of pallidum (L)	0.303	0.022
T1	Volume of hippocampus (L)	0.264	0.023
T1	Volume of amygdala (L)	0.224	0.019
T1	Volume of accumbens-area (L)	0.237	0.022
T1	Volume of ventral DC (L)	0.312	0.028
T1	Estimated total intracranial volume	0.175	0.022
T1	Total surface area (L)	0.314	0.024
T1	Global mean thickness (L)	0.211	0.021
DTI	Weighted-mean FA in tract acoustic radiation (L)	0.214	0.021
DTI	Weighted-mean FA in tract anterior thalamic radiation (L)	0.284	0.024
DTI	Weighted-mean FA in tract cingulate gyrus part of cingulum (L)	0.192	0.020
DTI	Weighted-mean FA in tract parahippocampal part of cingulum (L)	0.150	0.019
DTI	Weighted-mean FA in tract corticospinal tract (L)	0.194	0.021
DTI	Weighted-mean FA in tract forceps major	0.223	0.023
DTI	Weighted-mean FA in tract forceps minor	0.327	0.028
DTI	Weighted-mean FA in tract inferior fronto-occipital fasciculus (L)	0.264	0.027
DTI	Weighted-mean FA in tract inferior longitudinal fasciculus (L)	0.270	0.028
DTI	Weighted-mean FA in tract middle cerebellar peduncle	0.112	0.021
DTI	Weighted-mean FA in tract medial lemniscus (L)	0.146	0.023
DTI	Weighted-mean FA in tract posterior thalamic radiation (L)	0.222	0.023
DTI	Weighted-mean FA in tract superior longitudinal fasciculus (L)	0.328	0.027
DTI	Weighted-mean FA in tract superior thalamic radiation (L)	0.250	0.025
DTI	Weighted-mean FA in tract uncinate fasciculus (L)	0.232	0.023
fMRI	Net25 node 1 (default mode network incl. cerebellum)	0.119	0.017
fMRI	Net25 node 3 (temporal network)	0.105	0.017
fMRI	Net25 node 5 (right lateral network)	0.127	0.018
fMRI	Net25 node 6 (left lateral network)	0.140	0.017
fMRI	Net25 node 9 (temporoparietal network)	0.109	0.018
fMRI	Net25 node 13 (left ventral network)	0.168	0.020
fMRI	Net25 node 15 (cerebellar network)	0.113	0.016
fMRI	Net25 node 16 (prefrontal network)	0.104	0.019
fMRI	Net25 node 18 (subcortical network)	0.103	0.015
fMRI	Net25 node 20 (default mode network)	0.107	0.017
fMRI	Net25 node 21 (right ventral network)	0.110	0.018

Abbreviations: h^2 = SNP heritability; SE = standard error; L = left hemisphere of the brain; FA = fractional anisotropy; Net25 = 25-dimensional network; DTI = diffusion tensor imaging; fMRI = functional magnetic resonance imaging.

6 (WP6) of the European Network of National Schizophrenia Networks studying Gene-Environment

Interactions (EU-GEI).^{49,50} This dataset comprised 1525 healthy controls, 1261 individuals with schizophrenia, and 1282 healthy siblings of these patients. Our analysis focused solely on the group of healthy controls and individuals with a diagnosis of schizophrenia. The inclusion criteria for all individuals were (1) White European ancestry, (2) complete genetic and phenotype data, (3) originating from different families, and (4) genetically unrelated to each other (see below). Following these criteria, our final sample included 1065 individuals with schizophrenia (mean [SD] age 33.703 [8.650] years, 32.3% female) and 1037 healthy controls (mean [SD] age 34.187 [10.419] years, 48.5% female). The EU-GEI project received approval from the Medical Ethics Committees of 25 participating sites in 15 countries and was conducted in accordance with the Declaration of Helsinki. All participants in this study provided their written informed consent.⁵¹

GWAS Data Preprocessing

In this study, we focused exclusively on autosomal SNPs. Therefore, for GWAS that included sex chromosome SNPs, all such SNPs were removed from the analysis. Furthermore, SNPs within the extended major histocompatibility complex (MHC) region (chr6: 26000000-34000000) were removed from all GWAS data to mitigate potential bias arising from the intricate disequilibrium (LD) patterns.

Global-Level Genetic Overlap

Linkage Disequilibrium Score Regression For each pair of schizophrenia and brain imaging measures, we employed LDSC to evaluate the genome-wide genetic correlation,^{24,52} using pre-computed LD scores from 1000 Genomes European populations. Our analysis was restricted to markers overlapping with 1.2 million SNPs identified in the HapMap Project Phase 3⁵³ to minimize bias due to variable imputation quality. The Benjamini-Hochberg false discovery rate (FDR) procedure was applied to adjust for multiple comparisons across genetic correlations between schizophrenia and all examined imaging measures.

Polygenic Score PGS analysis was conducted utilizing the SBayesRC (v0.2.6) toolbox.⁵⁴ Duplicate and ambiguous SNPs were removed from each UKB brain GWAS dataset. Comprehensive details regarding imputation and quality control processes of the EU-GEI WP6 genotype data were documented in a previous publication.⁴⁹ We excluded variants with minor allele frequency below 0.01, and removed 1 individual from each pair of participants with a genetic relatedness coefficient greater than 0.125. After these quality control steps, 9 278 968

SNPs remained for PGS calculation in 2176 samples. SBayesRC was then employed to compute PGS for individuals in the EU-GEI WP6 dataset, based on the UKB brain GWAS. This method integrates functional genomic information with GWAS effect size to improve the estimation of SNP effect size and enhance the predictive performance of PGS. We utilized the functional genomic information for approximately 8 million SNPs, as provided by the developer, to refine the signal. Finally, logistic regression was performed to estimate the association between brain-based PGS and schizophrenia diagnosis. Sex, age, and the first 20 genetic principal components were included as covariates to control for potential confounding factors. The regression coefficient was used to assess the relationship between PGS and the diagnosis of schizophrenia.

Bivariate MiXeR The bivariate MiXeR analysis was applied to evaluate the polygenic overlap between schizophrenia and each brain imaging phenotype, regardless of genetic correlation.³⁹ MiXeR modeled the genetic effect on 2 traits through 4 bivariate Gaussian components, representing variants with no effect on either trait, variants with effect only on one trait, variants with effect on the other trait, and variants with effect on both traits. Through this model, MiXeR estimates the total number of shared and trait-specific causal variants, and the proportion of shared variants with concordant effect directions, meaning these variants simultaneously increase or decrease both traits. The Akaike Information Criterion (AIC) serves as a criterion for model fitting, with a positive AIC indicating that the Gaussian mixture model better fits the input data than a baseline infinitesimal model.

Local Genetic Overlap

To assess local genetic overlap and identify shared genetic loci between schizophrenia and brain imaging phenotypes, we utilized the conjFDR method from the pleioFDR toolbox.⁴⁰ This approach integrates conditional FDR (condFDR) analyses across 2 phenotypes to pinpoint specific genetic variants associated with both traits. For each schizophrenia-brain phenotype pair, it re-ranks the test statistics of variants for one phenotype based on their association strength with the other phenotype, and vice versa. The conjFDR value, defined as the maximum of the 2 condFDR statistics, represents an estimate of the posterior probability that a given SNP is not associated with either trait, under the condition that the P -values for that SNP in both traits are as small or smaller than the observed. This method is agnostic to the detection of the effects of overlapping SNP associations. Variants within the MHC region were excluded, and shared genetic variants were identified at a conjFDR threshold of $P < .05$.

Gene Mapping and Enrichment Analysis

For each shared locus identified by conjFDR, we selected the lead variant with the most significant conjFDR value. Subsequently, using the Variant-to-Gene pipeline from Open Targets Genetics,⁵⁵ these lead variants were assigned to genes based on the strongest evidence from 4 main data sources: molecular phenotypes from quantitative trait loci experiments, chromatin interaction experiments, in silico functional prediction, and proximity of each variant to the canonical transcription start site of genes. We conducted enrichment analysis on a subset of unique genes selected from all identified genes, comparing them against Gene Ontology (GO) terms^{56,57} and Kyoto Encyclopedia of Genes and Genomes (KEGG) pathways.^{58–60} To assess the significance of enrichment, we employed a hypergeometric distribution test using an R package “limma.”⁶¹ Furthermore, we applied the Benjamini-Hochberg FDR procedure to adjust for multiple tests. We also performed tissue specificity analysis through the Functional Mapping and Annotation GENE2FUNC module.⁶² Specifically, hypergeometric tests were employed to assess whether the identified unique genes were significantly enriched with the differentially expressed genes across the 54 tissue types profiled in the Genotype-Tissue Expression (GTEx) v8 database.⁶³

Statistical Analysis

To examine the relationship between global genetic correlation metrics, we calculated Pearson correlations among the genetic overlap metrics obtained from LDSC, PGS, and MiXeR. To determine which neuroimaging modalities have greater genetic overlap with schizophrenia, we compared the number of shared variants and loci across T1, DTI, and rs-fMRI using the Wilcoxon rank-sum test. A sensitivity analysis was performed on brain measures with positive AIC values from bivariate MiXeR analysis. The Benjamini-Hochberg FDR method was applied to correct for multiple comparisons. All statistical analyses were performed using R version 4.3.1, and the ggplot2 package was used for the visualization of all results.⁶⁴

Results

Global-Level Genetic Overlap

Linkage Disequilibrium Score Regression We first investigated the global genetic correlation between schizophrenia and various brain measures using LDSC. For T1 measures, genetic correlation ranged from -0.081 for the volume of ventral DC ($P_{\text{FDR}} = .069$) to 0.029 for total surface area ($P_{\text{FDR}} = .657$). For the DTI brain measures (mean FA), the correlations ranged from -0.099 for the forceps major ($P_{\text{FDR}} = .069$) to 0.031 for the parahippocampal part of the cingulum ($P_{\text{FDR}} = .711$). Functional MRI correlations spanned from -0.131 for

the subcortical network ($P_{\text{FDR}} = .069$) to 0.146 for the left lateral network ($P_{\text{FDR}} = .019$) (Figure 1A and Table S1). Overall, we found small correlations and only the left lateral network passed multiple comparisons correction.

Polygenic Score The logistic regression analysis revealed that the PGS for all the brain measures showed no significant associations with schizophrenia (Figure 1B). The regression coefficient for T1 structural brain measures ranged from -0.285 ($P_{\text{FDR}} = .788$) for the volume of amygdala to 0.370 ($P_{\text{FDR}} = .462$) for the global mean thickness. For DTI brain measures, mean FA in the middle cerebellar peduncle and medial lemniscus exhibited the strongest negative and positive correlation with schizophrenia, respectively ($\beta = -.620$, $P_{\text{FDR}} = .757$; $\beta = 3.666$, $P_{\text{FDR}} = .677$). Regarding the functional network, the PGS of the right lateral network and temporoparietal network displayed the strongest negative ($\beta = -4.931$, $P_{\text{FDR}} = .757$) and positive ($\beta = 8.417$, $P_{\text{FDR}} = .383$) correlation with schizophrenia (Table S2).

Bivariate MiXeR The bivariate MiXeR analysis uncovered a substantial amount of overlap of variants associated with schizophrenia and brain measures, as illustrated in Figure 1C and D, and Table S4. For the T1 brain measures, the global mean thickness measure demonstrated the most substantial overlap with schizophrenia, with 95.5% of variants shared (1243 out of 1302 variants), in contrast to total ICV, which had the least overlap at 11.4% (84 out of 737 variants). For DTI brain measures, the shared variant proportion ranged from 93.1% in the cingulate gyrus part of the cingulum (1658 out of 1780 variants) to 12.1% in the medial lemniscus (252 out of 2075 variants). For rs-fMRI measures, the proportion of shared variants with schizophrenia variants varied from 93.3% in the default mode network (735 out of 788 variants) to 24.8% in the prefrontal network (418 out of 1690 variants). Across 3 neuroimaging modalities, we also observed a varied proportion of shared variants with concordant effect directions (Figure 1C and Table S4). This proportion ranged between 0.317 and 0.520 (mean 0.460) for T1, and from 0.237 to 0.502 for DTI, with a mean of 0.392. The most variability was seen in rs-fMRI brain measures, ranging from 0.144 to 0.814, averaging 0.542. These findings highlight substantial genetic overlap among all the brain measures, although the shared variants show mixed directions of effect.

We calculated correlations between genetic overlap metrics across all examined brain measures. Notably, we observed a significant positive correlation between global genetic correlation and the regression coefficient of brain PGS with schizophrenia diagnosis ($r = 0.563$, $P_{\text{FDR}} = .001$) (Figure 2A). These 2 genetic overlap metrics both showed a significant positive correlation with the proportion of shared variants with concordant effect direction ($r = 0.779$, $P_{\text{FDR}} < .001$; $r = 0.394$, $P_{\text{FDR}} = .032$)

(Figure 2D and E). Additionally, T1 brain measures exhibited a significantly higher number of shared variants with schizophrenia compared to DTI brain measures ($P_{\text{FDR}} = .038$) (Figure S2). Excluding brain measures with negative AIC value, we still found a positive correlation between global genetic correlation and the sign-concordant rate of shared variants, and more shared variants with schizophrenia in T1 brain measures than in DTI (Table S5), underscoring the robustness of these findings.

Local-Level Genetic Overlap

ConjFDR analysis was used to identify specific shared variants between schizophrenia and brain measures. Based on $\text{conjFDR} < 0.05$, we identified 380 loci shared between schizophrenia and all the brain measures. The number of shared loci was between 4 and 37 for T1 measures (total of 218), between 2 and 22 for DTI measures (total of 138), and between 0 and 4 for rs-fMRI measures (total of 24) (Figure 3 and Table S6). Among these shared loci, 36 lead variants were jointly associated with schizophrenia and at least 2 brain measures (Table S7), resulting in 320 unique lead variants. Among the 3 neuroimaging modalities, T1 brain measures showed the greatest number of shared loci, whereas functional MRI had the fewest (Figure S2).

Gene Mapping and Enrichment Analysis

We conducted functional annotation by mapping the overlapping loci, identified through conjFDR, to genes through OpenTargets. This process identified 372 genes common to schizophrenia and each brain measure (Table S6), with 219 being unique. Specifically, schizophrenia shared 151 unique genes with T1 brain measures, 57 with DTI, and 11 with rs-fMRI measures. Of these shared genes, 62 were linked to schizophrenia and at least 2 brain measures, with 22 associated with both schizophrenia and the T1 and DTI brain measures (Table S8). In subsequent enrichment analysis, genes uniquely associated with both schizophrenia and T1 brain measures showed significant enrichment in the intracellular anatomical structure category ($P_{\text{FDR}} = .022$) (Table S9). However, genes uniquely shared between schizophrenia and DTI or rs-fMRI brain measures did not show enrichment in any GO categories and KEGG pathways. Conversely, genes common to schizophrenia and all studied brain measures were enriched for the GO domains molecular function and cellular components, specifically molecular function ($P_{\text{FDR}} = .047$), protein binding ($P_{\text{FDR}} = .038$), cell adhesion molecule (CAM) binding ($P_{\text{FDR}} = .047$), and postsynaptic density ($P_{\text{FDR}} = .047$) (Figure 4A and Table S10). Furthermore, the tissue-specific expression of all mapped genes was primarily concentrated in brain tissues, particularly in the putamen, hippocampus, and

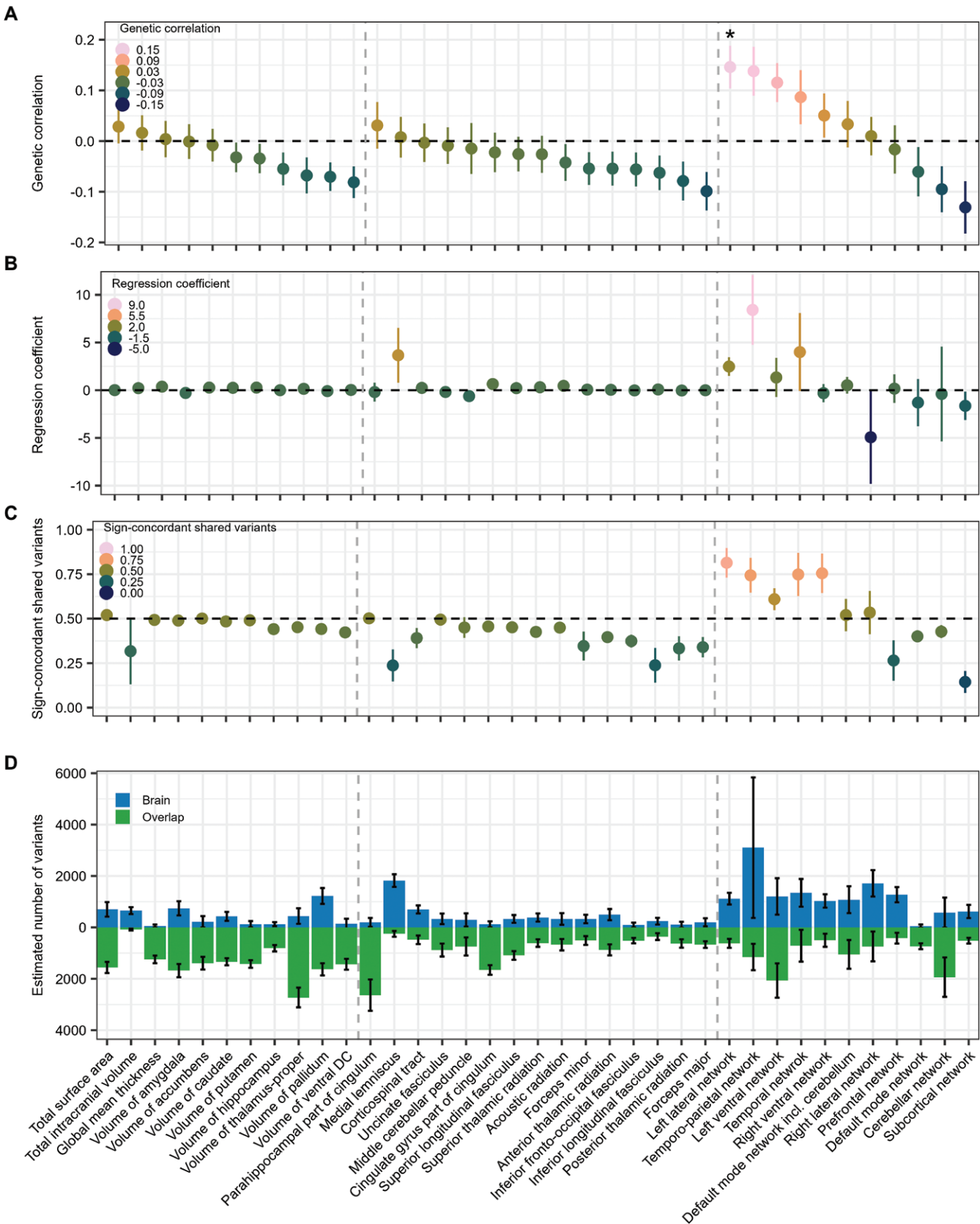


Figure 1. Genetic Overlap Between Schizophrenia and Brain Phenotypes at the Global Level. (A) Genetic correlation estimates. Using LDSC, we calculated the genetic correlation between schizophrenia and brain phenotypes. (B) Regression analysis. Estimated regression coefficients between polygenic scores for brain phenotypes and the diagnosis of schizophrenia. (C) The proportion of sign-concordant

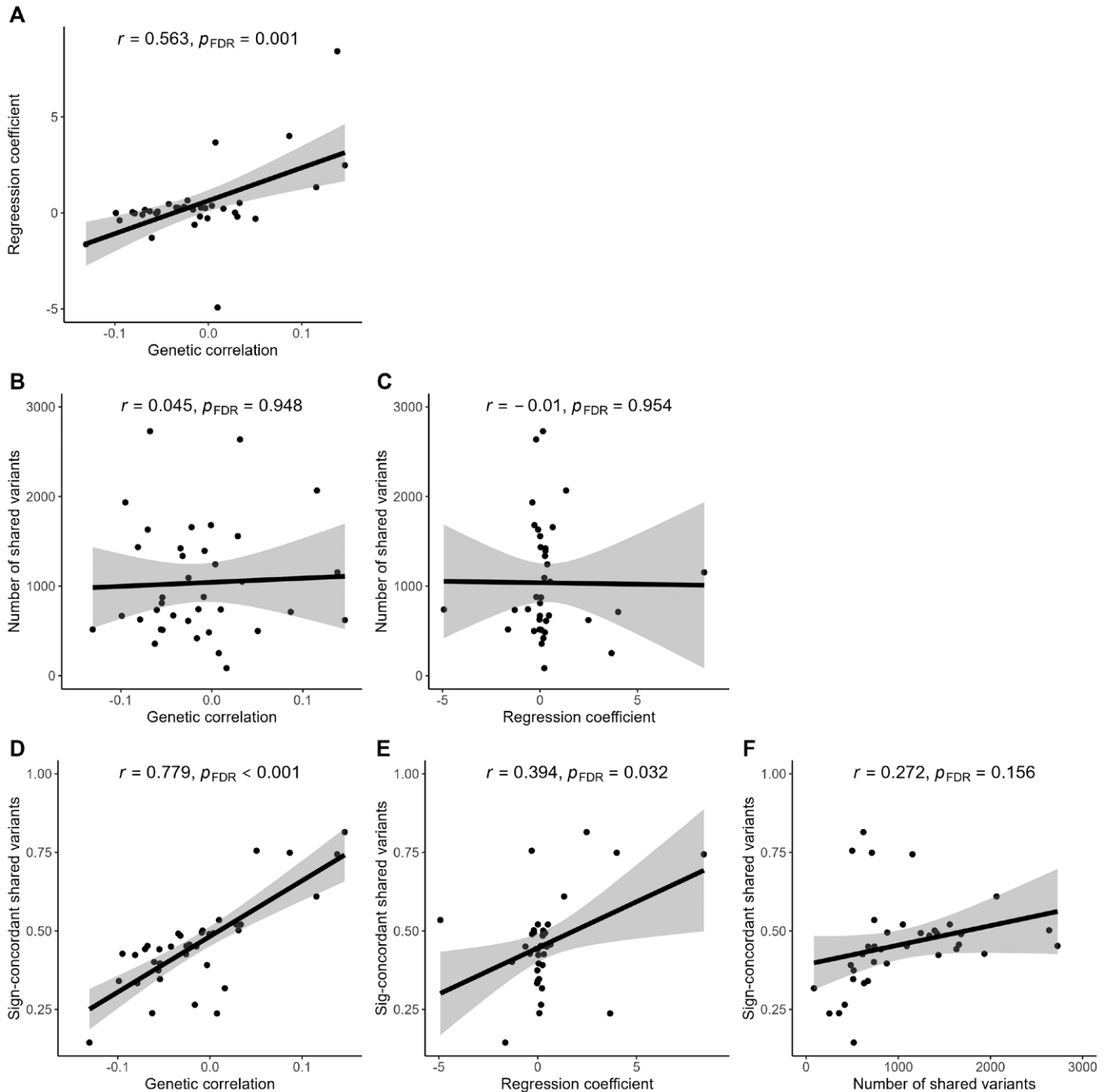


Figure 2. Correlation Between Metrics of Genetic Overlap. We calculated the correlation between different genetic overlap metrics, obtained from LDSC, polygenic score, and bivariate MiXeR. Each point represents an individual pairwise analysis between schizophrenia and a brain phenotype. The P -values adjusted for multiple comparisons (P_{FDR}) are shown. Abbreviations: FDR = false discovery rate; LDSC = linkage disequilibrium score regression.

shared variants. We estimated the proportion of shared variants with concordant effect direction between schizophrenia and brain phenotypes using bivariate MiXeR. (D) The number of trait-specific and shared causal variants. Bivariate MiXeR modeling the shared (green) and brain phenotypes-specific (blue) causal variants. Error bars reflect standard error in plot A, and reflect standard deviation in plots B, C, and D. Asterisks (*) in plot A signify statistical significance ($P < .05$) after multiple comparisons correction for 37 brain measures. The vertical gray dashed lines separate the brain measures according to the modalities. Specific brain measures from T1 and DTI are located in the left hemisphere; refer to [Table S1](#) for details. Complete details of this figure are provided in [Tables S1-S4](#). Abbreviations: DTI = diffusion tensor imaging; LDSC = linkage disequilibrium score regression.

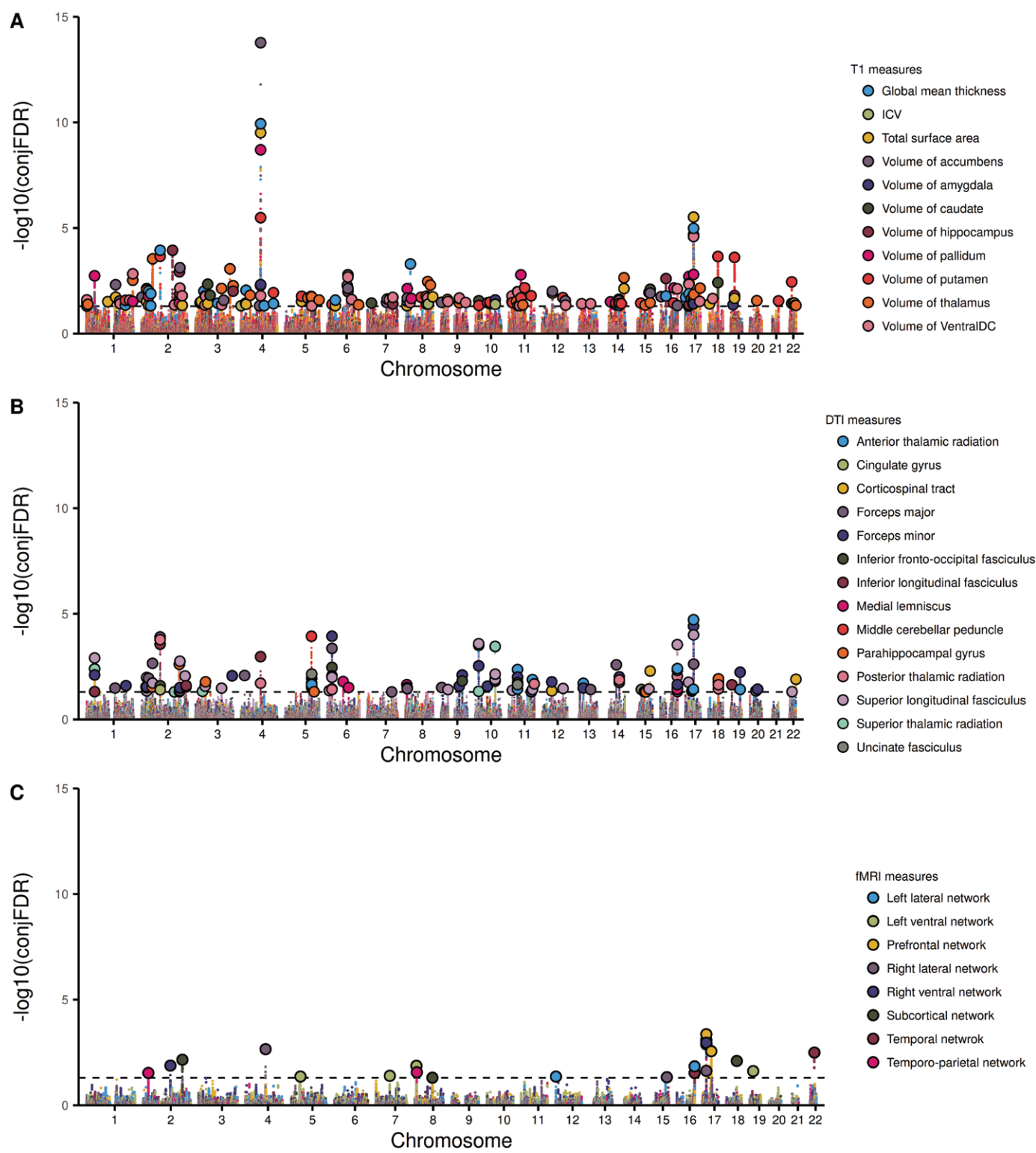


Figure 3. Shared Genetic Loci Between Schizophrenia and Brain Imaging Phenotypes. The x-axis reflects the chromosomal position, and the y-axis shows the $-\log_{10}$ transformed conjugal false discovery rate (conjFDR). Each dot represents an SNP; lead SNPs of shared loci are indicated by a bold border. Different colors correspond to different brain imaging phenotypes. The horizontal dotted line marks the significant threshold ($-\log_{10}(0.05)$). Panels A, B, and C illustrate the shared loci identified with T1, DTI, and fMRI, respectively. Abbreviations: DTI = diffusion tensor imaging; fMRI = functional magnetic resonance imaging.

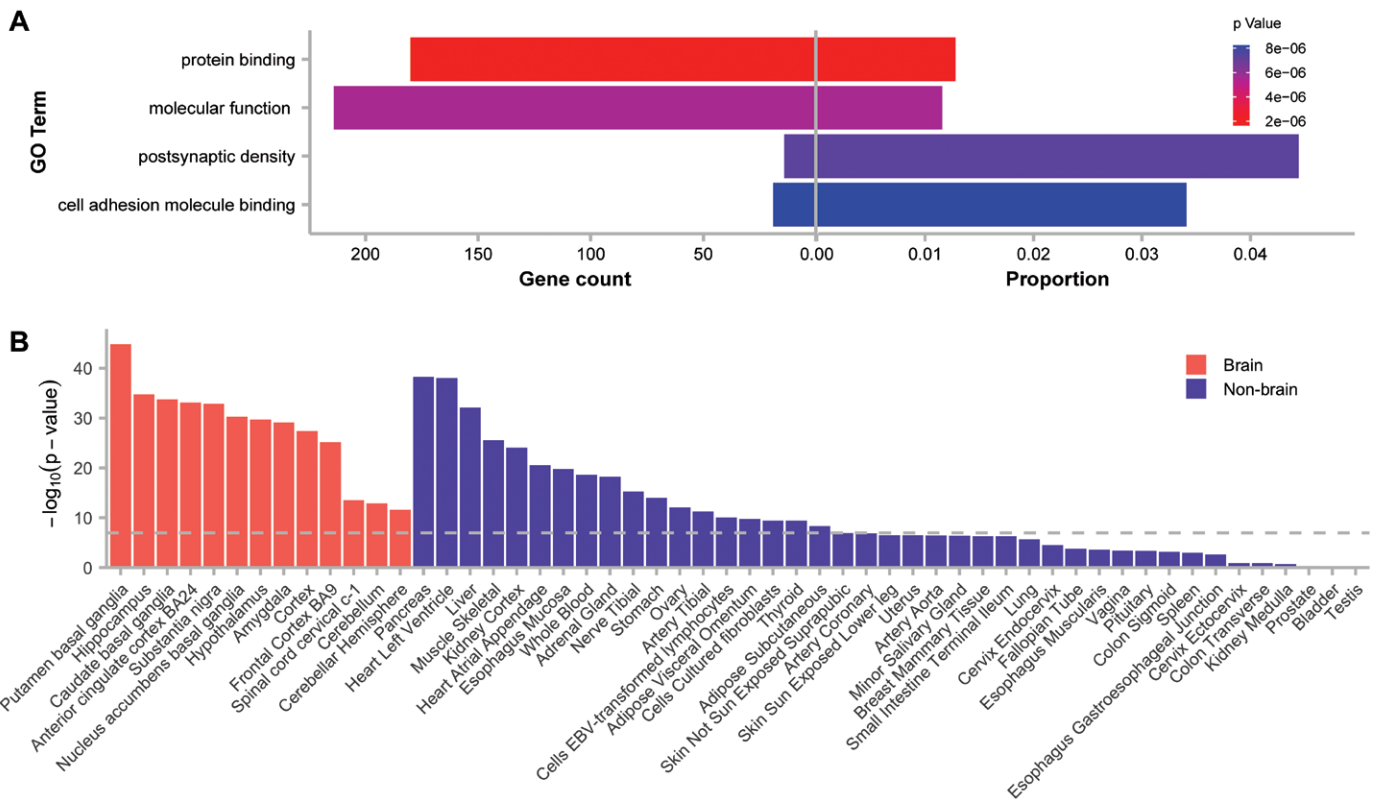


Figure 4. Enrichment Analysis and Tissue Specificity Analysis for Genes Mapped to Conjunctive FDR Loci. (A) Enrichment analysis of the mapped genes. The left bar shows the count of genes overlapping between schizophrenia and all brain phenotypes. The right bar indicates the proportion of the number of overlapped genes and the total genes in the gene sets. All depicted results have survived correction for multiple comparisons. (B) Tissue-specific expression of the mapped genes. The y-axis represents the $-\log_{10}(P\text{-value})$ of differential gene expression in each tissue type, and the x-axis represents the 54 tissues from the GTEx v8 database, grouped into brain and nonbrain tissues. The horizontal dashed line indicates the significance threshold after Bonferroni correction ($P_{\text{FDR}} = .05/54$ tissues). Abbreviation: FDR = false discovery rate.

caudate, as well as in several nonbrain tissues, including the pancreas, heart, and liver (**Figure 4B**). This expression pattern is consistent with expectation, given that these genes were identified based on shared relevance to both schizophrenia and brain phenotypes.

Discussion

We investigated the shared genetic architecture between schizophrenia and 37 brain neuroimaging phenotypes from T1-weighted, diffusion MRI, and rs-fMRI and found a substantial number of shared variants. Using multiple statistical methods, we provide complementary insights into the intricate genetic overlap with mixed effect direction at both genome-wide and individual locus levels. While this complex shared genetic architecture is not fully discernible using LDSC and PGS alone, the observed positive correlations among LDSC-derived genetic correlation, PGS regression coefficients, and MiXeR-derived proportion of sign-concordant shared variants underscored the continued value of these approaches in exploring genetic overlap. These findings highlight the necessity of a multifaceted approach for comprehensively

characterizing genetic overlap between polygenic phenotypes. Furthermore, our gene-level analysis of mapped genes revealed significant enrichment in molecular function gene sets, including protein binding, CAM binding, and postsynaptic density, as well as brain-specific expression profiles.

Using MiXeR and conjFDR, we found extensive genetic overlap between schizophrenia and all brain imaging phenotypes at genome-wide and individual locus levels. This overlap, coupled with previous neuroimaging evidence demonstrating distinct group differences in brain measures,^{8,9,13} suggests that the genetic architecture of schizophrenia and brain phenotypes is not independent and that at least some of the group differences in brain phenotypes are genetically determined. Additionally, the extensive genetic overlap was observed in scenarios of weak genetic correlation, concordant with earlier studies,^{20,21} implying a balance of shared genetic variance with both consistent and opposing effect directions on schizophrenia and brain phenotypes. Consequently, the shared genetic variants that are involved in brain phenotypes may have both risk-enhancing and risk-reducing effects on schizophrenia.²⁸ Overall, building on prior

findings, we expand the scope to include T1, DTI, and rs-fMRI brain neuroimaging phenotypes, demonstrating that schizophrenia shares a genetic basis with the brain's morphology, white matter microstructure, and resting-state functional activity.

Diverse methodologies allow us to dissect the shared genetic architecture between schizophrenia and brain imaging phenotypes from different perspectives. LDSC captures average genetic signals across the genome and reveals weak or no genetic correlations between schizophrenia and brain phenotypes—findings consistent with prior studies.^{21,23,25,26} These results underscore LDSC's limitations in addressing the complexity of mixed effect directions among shared variants. PGS, which aggregates genome-wide causal variants to infer genetic relationships between 2 traits,^{65,66} showed insignificant associations between brain measures and schizophrenia, likely due to its struggles in detecting genetic overlap when shared variants have opposing effects. In contrast, bivariate MiXeR is unaffected by the directionality of effects in shared variants³⁹ and identified numerous brain- and schizophrenia-specific and shared variants, noting a significant proportion of sign-concordant shared variants consistent with earlier studies.^{21,22,26,28} Importantly, global genetic correlation and regression coefficient of PGS had a significant positive correlation with the proportion of sign-concordant shared variants, rather than the number of shared variants. This finding challenges the traditional assumption that higher genetic correlation or regression coefficient of PGS necessarily implies greater genetic overlap,²⁰ suggesting instead that these 2 methodologies capture only or mainly part of the genetic overlap with consistent effects on both traits. Finally, conjFDR identified hundreds of loci shared between schizophrenia and brain phenotypes, offering insights into the biological mechanisms underlying their shared genetic basis.

While there was extensive genetic overlap between schizophrenia and all examined brain measures, the extent of shared causal variants and loci varied across different imaging modalities. Specifically, T1 brain measures demonstrated more shared genetic variants and loci with schizophrenia than DTI and rs-fMRI. This observation could be attributed to the higher SNP-based heritability of T1 brain measures observed in our study, in line with previous research,⁴³ indicating a stronger genetic influence on the brain's morphological structure. Additionally, T1 measurements typically exhibit lower noise levels compared to DTI and rs-fMRI, potentially leading to more reliable genetic associations. Furthermore, our observation aligns with findings from multivariate GWAS analyses of brain imaging phenotypes, which indicated few loci and genes associated with rs-fMRI and DTI brain measurements compared to T1.⁴³ Based on these findings, we speculate that structural aspects of the brain, especially morphological features captured by T1 structure, may be more closely related to the genetic underpinnings of schizophrenia than brain functions captured

by rs-fMRI. However, further investigation is necessary to confirm this speculation and explore the underlying mechanisms.

Among the genes mapped via shared SNPs identified by conjFDR, several have been previously associated with schizophrenia. Notably, *ACTR1B* encodes a subunit of dynein complex involved in microtubule remodeling and neuronal migration,⁶⁷ and has been associated with mean cortical thickness.¹⁸ Its overlap with both schizophrenia and mean cortical thickness, and mean FA across multiple white matter tracts, suggests a potential involvement in cortex structural organization and white matter integrity, which are commonly implicated in schizophrenia-related neuropathology.^{7,9} *BCL11B* is a zinc-finger transcription factor essential for establishing and maintaining neuronal connections during central nervous system development.⁶⁸ *CACNA1C*, encoding a subunit of L-type calcium channel,⁶⁹ is crucial for neuronal excitability, synaptic plasticity, and normal brain development.⁷⁰ *GATAD2A* encodes a component of the NuRD (nucleosome remodeling and deacetylase) complex involved in regulating cell-cycle progression, genome integrity, and cellular differentiation.⁷¹ The above 3 genes have all been implicated in neurodevelopmental processes. Our findings provide additional cues that these genes may affect cortical architecture and functional connectivity during brain development and thus contribute to schizophrenia pathology. *EPN2* was mapped through shared variants between schizophrenia and multiple functional networks. It has been prioritized in schizophrenia GWAS using fine-mapping and protein-protein interaction integrated analyses, supporting its potential causal role.⁷² Given *EPN2*'s role in synaptic vesicle endocytosis,⁷³ genetic variations in this gene may disrupt efficient neurotransmission, potentially leading to altered large-scale brain network connectivity observed in schizophrenia.^{12,13}

The enrichment analysis of GO and KEGG revealed that genes shared between schizophrenia and all brain measures were enriched for protein binding, particularly CAM binding, implicating their roles in synaptic plasticity and function.⁷⁴ Altered CAM levels and the PGS of the CAM pathway have been associated with impairments in memory and attention in schizophrenia.^{75–77} Our findings thus add support to the hypothesis that CAM plays a key role in the pathophysiology of schizophrenia. Additionally, enrichment of the postsynaptic density gene set aligns with prior evidence of reduced postsynaptic density in schizophrenia⁷⁸ and reinforces the hypothesis that schizophrenia may fundamentally involve disruptions in brain connectivity.¹² Tissue-specific expression analysis showed significant enrichment in brain tissues, especially subcortical regions such as the putamen, caudate, and hippocampus, consistent with known structural abnormalities in schizophrenia.^{8,79} Enrichment in cortical regions, including the frontal cortex and anterior cingulate cortex, further supports the view that schizophrenia involves widespread disruptions across multiple

brain networks.¹³ Additionally, the observed enrichment in nonbrain tissues, such as the heart and liver, may reflect broader gene regulatory networks or developmental co-expression patterns, wherein neurodevelopment genes are also active in other tissues during early development.²¹

This study has several limitations. First, our analyses were limited to samples of European ancestry, and brain phenotypes are from the UK Biobank, a cohort with participants aged 45-76. Thus, the generalizability of our findings to other age groups and populations remains to be established. Second, the limited statistical power in some brain GWAS did not warrant the use of the bivariate MiXeR model. However, excluding brain phenotypes with negative AIC values did not alter the significant correlations between MiXeR-derived and other genetic overlap metrics, supporting the robustness of our findings. Third, conjFDR and PGS association analyses depend on the power of input GWASs, which is largely determined by sample size. Similarly, previously inconsistent genetic correlation results may also be attributed to limited GWAS sample size.^{20,21,23} Larger cohorts will improve precision and power to detect genetic overlap through these approaches. Fourth, the brain GWAS summary statistics used were not uniformly adjusted for ICV or other global brain measures, potentially confounding region-specific associations with global brain size effects. Future work using raw imaging data and GWAS conditioned on global measures is needed. Fifth, we examined a limited set of brain measures and restricted analyses to the left hemisphere for bilateral brain phenotypes, which may limit the detection of additional shared variants with schizophrenia. Broader phenotypic coverage is warranted in further studies. Finally, other methods, such as colocalization analysis,⁸⁰ could further test shared causal variants between 2 traits, while multivariate approaches like the Multivariate Omnibus Statistical Test⁸¹ may enhance the discovery of genetic variants with distributed effects across a set of related measures.^{43,82-84} Applying these approaches may provide deeper insights into the genetic overlap between schizophrenia and brain phenotypes, and could be extended to other disease-related traits, such as psychiatric or behavioral phenotypes, as a valuable avenue for future investigation.

To conclude, we found extensive polygenic overlap with mixed effect direction between schizophrenia and the brain neuroimaging phenotypes at the genome-wide and individual locus levels. Our findings highlight the importance of exploring different methodologies in studying the genetic overlap of complex traits and provide complementary insight into the shared genetic basis between schizophrenia and brain morphology, white matter microstructure, and functional connectivity.

Supplementary material

Supplementary material is available at <https://academic.oup.com/schizophreniabulletin>.

Acknowledgments

This research was made possible, in part, using the Data Science Research Infrastructure (DSRI), hosted at Maastricht University.

Author contributions

X.W. and D.v.d.M. conceived the study. B.D.L. and L.-K.P. preprocessed part of the data. X.W. performed all analyses and drafted the manuscript. All authors contributed to reviewing and editing the final manuscript.

Funding

This work was supported by the Research Council of Norway (#324252 and #324499); Nordforsk (#164218); the European Union's Horizon 2020 research and innovation program under the Marie Skłodowska-Curie (801133); the China Scholarship Council (CSC) scholarship from the Ministry of Education of P.R. China and the YOUTH -GEMs project funded by the European Union's Horizon Europe program (101057182).

Conflicts of interest

O.A.A. is a consultant to Cortechs.ai and Precision Health AI and has received speaker's honorarium from Lundbeck, Janssen, Sunovion, and Otsuka. All other authors report no biomedical financial interests or potential conflicts of interest.

Data availability

The data incorporated in this work were gathered from public resources and the EU-GEI study.

References

1. Trubetskoy V, Pardiñas AF, Qi T, et al; Indonesia Schizophrenia Consortium. Mapping genomic loci implicates genes and synaptic biology in schizophrenia. *Nature*. 2022;604:502–508.
2. Solmi M, Seitidis G, Mavridis D, et al. Incidence, prevalence, and global burden of schizophrenia - data, with critical appraisal, from the Global Burden of Disease (GBD) 2019. *Mol Psychiatry*. 2023;28:5319–5327.
3. McCutcheon RA, Marques TR, Howes OD. Schizophrenia—an overview. *JAMA Psychiatry*. 2020;77:201–210.
4. Rapoport JL, Addington AM, Frangou S, Psych MRC. The neurodevelopmental model of schizophrenia: update 2005. *Mol Psychiatry*. 2005;10:434–449.
5. Okada N, Fukunaga M, Yamashita F, et al. Abnormal asymmetries in subcortical brain volume in schizophrenia. *Mol Psychiatry*. 2016;21:1460–1466.
6. Rimol LM, Hartberg CB, Nesvåg R, et al. Cortical thickness and subcortical volumes in schizophrenia and bipolar disorder. *Biol Psychiatry*. 2010;68:41–50.

7. Erp TGM van, Walton E, Hibar DP, et al. Cortical brain abnormalities in 4474 individuals with schizophrenia and 5098 control subjects via the Enhancing Neuro Imaging Genetics Through Meta Analysis (ENIGMA) Consortium. *Biol Psychiatry*. 2018;84:644–654.
8. Erp TGM van, Hibar DP, Rasmussen JM, et al. Subcortical brain volume abnormalities in 2028 individuals with schizophrenia and 2540 healthy controls via the ENIGMA Consortium. *Mol Psychiatry*. 2016;21:547–553.
9. Kelly S, Jahanshad N, Zalesky A, et al. Widespread white matter microstructural differences in schizophrenia across 4322 individuals: results from the ENIGMA Schizophrenia DTI Working Group. *Mol Psychiatry*. 2018;23:1261–1269.
10. Kanaan RAA, Kim JS, Kaufmann WE, Pearlson GD, Barker GJ, McGuire PK. Diffusion tensor imaging in schizophrenia. *Biol Psychiatry*. 2005;58:921–929.
11. Lee SH, Kubicki M, Asami T, et al. Extensive white matter abnormalities in patients with first-episode schizophrenia: a diffusion tensor imaging (DTI) study. *Schizophr Res*. 2013;143:231–238.
12. Narr KL, Leaver AM. Connectome and schizophrenia. *Curr Opin Psychiatry*. 2015;28:229–235.
13. Dong D, Wang Y, Chang X, Luo C, Yao D. Dysfunction of large-scale brain networks in schizophrenia: a meta-analysis of resting-state functional connectivity. *Schizophr Bull*. 2017;44:168–181.
14. Satizabal CL, Adams HHH, Hibar DP, et al. Genetic architecture of subcortical brain structures in 38,851 individuals. *Nat Genet*. 2019;51:1624–1636.
15. Miranda-Dominguez O, Feczko E, Grayson DS, Walum H, Nigg JT, Fair DA. Heritability of the human connectome: a connectotyping study. *Netw Neurosci*. 2018;2:175–199.
16. Kochunov P, Jahanshad N, Marcus D, et al. Heritability of fractional anisotropy in human white matter: a comparison of Human Connectome Project and ENIGMA-DTI data. *Neuroimage*. 2015;111:300–311.
17. Colclough GL, Smith SM, Nichols TE, et al. The heritability of multi-modal connectivity in human brain activity. *eLife*. 2017;6:e20178.
18. Grasby KL, Jahanshad N, Painter JN, et al; Alzheimer's Disease Neuroimaging Initiative. The genetic architecture of the human cerebral cortex. *Science*. 2020;367:eaay6690.
19. Camchong J, Lim KO, Sponheim SR, MacDonald AW. Frontal white matter integrity as an endophenotype for schizophrenia: diffusion tensor imaging in monozygotic twins and patients' nonpsychotic relatives. *Front Hum Neurosci*. 2009;3:35.
20. Franke B, Stein JL, Ripke S, et al; Schizophrenia Working Group of the Psychiatric Genomics Consortium. Genetic influences on schizophrenia and subcortical brain volumes: large-scale proof of concept. *Nat Neurosci*. 2016;19:420–431.
21. Cheng W, Meer D van der, Parker N, et al. Shared genetic architecture between schizophrenia and subcortical brain volumes implicates early neurodevelopmental processes and brain development in childhood. *Mol Psychiatry*. 2022;27:5167–5176.
22. Smeland OB, Wang Y, Frei O, et al. Genetic overlap between schizophrenia and volumes of hippocampus, putamen, and intracranial volume indicates shared molecular genetic mechanisms. *Schizophr Bull*. 2017;44:854–864.
23. Ohi K, Shimada T, Kataoka Y, et al. Genetic correlations between subcortical brain volumes and psychiatric disorders. *Br J Psychiatry*. 2020;216:280–283.
24. Bulik-Sullivan B, Finucane HK, Anttila V, et al; ReproGen Consortium. An atlas of genetic correlations across human diseases and traits. *Nat Genet*. 2015;47:1236–1241.
25. Roelfs D, Meer D van der, Alnæs D, et al. Genetic overlap between multivariate measures of human functional brain connectivity and psychiatric disorders. *Nat Ment Heal*. 2024;2:189–199.
26. Parker N, Cheng W, Hindley GFL, et al. Psychiatric disorders and brain white matter exhibit genetic overlap implicating developmental and neural cell biology. *Mol Psychiatry*. 2023;28:4924–4932.
27. Meer D van der, Frei O, Kaufmann T, et al. Quantifying the polygenic architecture of the human cerebral cortex: extensive genetic overlap between cortical thickness and surface area. *Cereb Cortex*. 2020;30:5597–5603.
28. Hindley G, Frei O, Shadrin AA, et al. Charting the landscape of genetic overlap between mental disorders and related traits beyond genetic correlation. *Am J Psychiatry*. 2022;179:833–843.
29. Neilson E, Bois C, Gibson J, et al. Effects of environmental risks and polygenic loading for schizophrenia on cortical thickness. *Schizophr Res*. 2017;184:128–136.
30. Neilson E, Shen X, Cox SR, et al. Impact of polygenic risk for schizophrenia on cortical structure in UK Biobank. *Biol Psychiatry*. 2019;86:536–544.
31. Harrisberger F, Smieskova R, Vogler C, et al. Impact of polygenic schizophrenia-related risk and hippocampal volumes on the onset of psychosis. *Transl Psychiatry*. 2016;6:e868–e868.
32. Liu S, Li A, Liu Y, et al. Polygenic effects of schizophrenia on hippocampal grey matter volume and hippocampus–medial prefrontal cortex functional connectivity. *Br J Psychiatry*. 2020;216:267–274.
33. Cao H, Zhou H, Cannon TD. Functional connectome-wide associations of schizophrenia polygenic risk. *Mol Psychiatry*. 2021;26:2553–2561.
34. Rashid B, Chen J, Rashid I, et al. A framework for linking resting-state connectome/genome features in schizophrenia: a pilot study. *Neuroimage*. 2019;184:843–854.
35. Yang X, Sullivan PF, Li B, et al. Multi-organ imaging-derived polygenic indexes for brain and body health. *medRxiv*. 2024:2023.04.18.23288769.
36. Lin BD, Li Y, Goula AA, et al. Dissecting causal relationships between cortical morphology and neuropsychiatric disorders: a bidirectional Mendelian randomization study. *Nat Ment Heal*. Published online 2025:1–13.
37. Guo J, Yu K, Dong SS, et al. Mendelian randomization analyses support causal relationships between brain imaging-derived phenotypes and risk of psychiatric disorders. *Nat Neurosci*. 2022;25:1519–1527.
38. Meer D van der, Hindley G, Shadrin A, et al. Mapping the genetic landscape of psychiatric disorders with the MiXeR toolset. *Biol Psychiatry*. 2025. advance online publication.
39. Frei O, Holland D, Smeland OB, et al. Bivariate causal mixture model quantifies polygenic overlap between complex traits beyond genetic correlation. *Nat Commun*. 2019;10:2417.
40. Andreassen OA, Thompson WK, Schork AJ, et al; Psychiatric Genomics Consortium (PGC). Improved detection of common variants associated with schizophrenia and bipolar disorder using pleiotropy-informed conditional false discovery rate. *PLoS Genet*. 2013;9:e1003455.
41. Andreassen OA, Djurovic S, Thompson WK, et al; International Consortium for Blood Pressure GWAS. Improved detection of common variants associated with

- schizophrenia by leveraging pleiotropy with cardiovascular-disease risk factors. *Am J Hum Genet.* 2013;92:197–209.
42. Roelfs D, Frei O, Meer D van der, et al. Shared genetic architecture between mental health and the brain functional connectome in the UK Biobank. *BMC Psychiatry.* 2023;23:461.
 43. Tisink EP, Shadrin AA, Meer D van der, et al. Abundant pleiotropy across neuroimaging modalities identified through a multivariate genome-wide association study. *Nat Commun.* 2024;15:2655.
 44. Smith SM, Douaud G, Chen W, et al. An expanded set of genome-wide association studies of brain imaging phenotypes in UK Biobank. *Nat Neurosci.* 2021;24:737–745.
 45. Guadalupe T, Mathias SR, vanErp TGM, et al. Human subcortical brain asymmetries in 15,847 people worldwide reveal effects of age and sex. *Brain Imaging Behav.* 2017;11:1497–1514.
 46. Shi H, Mancuso N, Spendlove S, Pasaniuc B. Local genetic correlation gives insights into the shared genetic architecture of complex traits. *Am J Hum Genet.* 2017;101:737–751.
 47. Elliott LT, Sharp K, Alfaro-Almagro F, et al. Genome-wide association studies of brain imaging phenotypes in UK Biobank. *Nature.* 2018;562:210–216.
 48. Alfaro-Almagro F, Jenkinson M, Bangerter NK, et al. Image processing and quality control for the first 10,000 brain imaging datasets from UK Biobank. *Neuroimage.* 2018;166:400–424.
 49. Guloksuz S, Pries L, Delespaul P, et al; Genetic Risk and Outcome of Psychosis (GROUP) Investigators. Examining the independent and joint effects of molecular genetic liability and environmental exposures in schizophrenia: results from the EUGEI study. *World Psychiatry.* 2019;18:173–182.
 50. Os J van, Rutten BP, et al.; (EU-GEI) EN of NN Studying GEI in S. Identifying gene-environment interactions in schizophrenia: contemporary challenges for integrated, large-scale investigations. *Schizophr Bull.* 2014;40:729–736.
 51. Os J van, Pries LK, Delespaul P, et al. Replicated evidence that endophenotypic expression of schizophrenia polygenic risk is greater in healthy siblings of patients compared to controls, suggesting gene-environment interaction. The EUGEI study. *Psychol Med.* 2020;50:1884–1897.
 52. Consortium SWG of the PG, Bulik-Sullivan BK, Loh PR, et al. LD score regression distinguishes confounding from polygenicity in genome-wide association studies. *Nat Genet.* 2015;47:291–295.
 53. Consortium IH, Altshuler DM, Gibbs RA, et al. Integrating common and rare genetic variation in diverse human populations. *Nature.* 2010;467:52–58.
 54. Zheng Z, Liu S, Sidorenko J, et al; LifeLines Cohort Study. Leveraging functional genomic annotations and genome coverage to improve polygenic prediction of complex traits within and between ancestries. *Nat Genet.* 2024;56:767–777.
 55. Mountjoy E, Schmidt EM, Carmona M, et al. An open approach to systematically prioritize causal variants and genes at all published human GWAS trait-associated loci. *Nat Genet.* 2021;53:1527–1533.
 56. Ashburner M, Ball CA, Blake JA, et al. Gene Ontology: tool for the unification of biology. *Nat Genet.* 2000;25:25–29.
 57. Aleksander SA, Balhoff J, Carbon S, et al; Gene Ontology Consortium. The Gene Ontology knowledgebase in 2023. *Genetics.* 2023;224:iyad031.
 58. Kanehisa M, Furumichi M, Sato Y, Kawashima M, Ishiguro-Watanabe M. KEGG for taxonomy-based analysis of pathways and genomes. *Nucleic Acids Res.* 2022;51:D587–D592.
 59. Kanehisa M, Goto S. KEGG: Kyoto Encyclopedia of Genes and Genomes. *Nucleic Acids Res.* 2000;28:27–30.
 60. Kanehisa M. Toward understanding the origin and evolution of cellular organisms. *Protein Sci.* 2019;28:1947–1951.
 61. Ritchie ME, Phipson B, Wu D, et al. limma powers differential expression analyses for RNA-sequencing and microarray studies. *Nucleic Acids Res.* 2015;43:e47–e47.
 62. Watanabe K, Taskesen E, Bochoven A van, Posthuma D. Functional mapping and annotation of genetic associations with FUMA. *Nat Commun.* 2017;8:1826.
 63. GTEx Consortium, Aguet F, Anand S, et al. The GTEx Consortium atlas of genetic regulatory effects across human tissues. *Science.* 2020;369:1318–1330.
 64. Wilkinson L. ggplot2: elegant graphics for data analysis by Wickham, H. *Biometrics.* 2011;67:678–679.
 65. Middeldorp CM, Moor MHM de, McGrath LM, et al. The genetic association between personality and major depression or bipolar disorder. A polygenic score analysis using genome-wide association data. *Transl Psychiatry.* 2011;1:e50–e50.
 66. Merwe C van der, Passchier R, Mufford M, Ramesar R, Dalvie S, Stein DJ. Polygenic risk for schizophrenia and associated brain structural changes: a systematic review. *Compr Psychiatry.* 2019;88:77–82.
 67. Schroer TA. Dynactin. *Annu Rev Cell Dev Biol.* 2004;20:759–779.
 68. Seigfried FA, Britsch S. The Role of Bcl11 transcription factors in neurodevelopmental disorders. *Biology.* 2024;13:126.
 69. Harrison PJ, Husain SM, Lee H, et al. CACNA1C (CaV1.2) and other L-type calcium channels in the pathophysiology and treatment of psychiatric disorders: advances from functional genomics and pharmacoepidemiology. *Neuropharmacology.* 2022;220:109262.
 70. Kabir ZD, Martínez-Rivera A, Rajadhyaksha AM. From gene to behavior: L-type calcium channel mechanisms underlying neuropsychiatric symptoms. *Neurotherapeutics.* 2017;14:588–613.
 71. Ma C, Gu C, Huo Y, Li X, Luo XJ. The integrated landscape of causal genes and pathways in schizophrenia. *Transl Psychiatry.* 2018;8:67.
 72. Hsu YHH, Pintacuda G, Liu R, et al; Schizophrenia Working Group of the Psychiatric Genomics Consortium. Using brain cell-type-specific protein interactomes to interpret neurodevelopmental genetic signals in schizophrenia. *iScience.* 2023;26:106701.
 73. Sen A, Madhivanan K, Mukherjee D, Aguilar RC. The epsin protein family: coordinators of endocytosis and signaling. *Biomol Concepts.* 2012;3:117–126.
 74. Sytnyk V, Leshchyn'ska I, Schachner M. Neural cell adhesion molecules of the immunoglobulin superfamily regulate synapse formation, maintenance, and function. *Trends Neurosci.* 2017;40:295–308.
 75. Cai HQ, Weickert TW, Catts VS, et al. Altered levels of immune cell adhesion molecules are associated with memory impairment in schizophrenia and healthy controls. *Brain Behav Immun.* 2020;89:200–208.
 76. Boiko AS, Mednova IA, Kornetova EG, Semke AV, Bokhan NA, Ivanova SA. Cell adhesion molecules in schizophrenia patients with metabolic syndrome. *Metabolites.* 2023;13:376.
 77. Hargreaves A, Anney R, O'Dushlaine C, et al; Schizophrenia Psychiatric Genome-Wide Association Study Consortium

- (PGC-SCZ). The one and the many: effects of the cell adhesion molecule pathway on neuropsychological function in psychosis. *Psychol Med*. 2014;44:2177–2187.
78. Berlekom AB van, Muflihah CH, Snijders GJJ, et al. Synapse pathology in schizophrenia: a meta-analysis of postsynaptic elements in postmortem brain studies. *Schizophr Bull*. 2019;46:374–386.
 79. Boos HBM, Aleman A, Cahn W, Pol HH, Kahn RS. Brain volumes in relatives of patients with schizophrenia: a meta-analysis. *Arch Gen Psychiatry*. 2007;64:297–304.
 80. Giambartolomei C, Vukcevic D, Schadt EE, et al. Bayesian test for colocalisation between pairs of genetic association studies using summary statistics. *PLoS Genet*. 2014;10:e1004383.
 81. Meer D van der, Frei O, Kaufmann T, et al. Understanding the genetic determinants of the brain with MOSTest. *Nat Commun*. 2020;11:3512.
 82. Meer D van der, Shadrin AA, O’Connell K, et al. Boosting schizophrenia genetics by utilizing genetic overlap with brain morphology. *Biol Psychiat*. 2022;92:291–298.
 83. Roelfs D, Meer D van der, Alnæs D, et al. Genetic overlap between multivariate measures of human functional brain connectivity and psychiatric disorders. *Nat Ment Heal*. 2024;2:189–199.
 84. Fan CC, Loughnan R, Makowski C, et al. Multivariate genome-wide association study on tissue-sensitive diffusion metrics highlights pathways that shape the human brain. *Nat Commun*. 2022;13:2423.